

1 **Extensive recombination-driven coronavirus diversification expands the pool of**
2 **potential pandemic pathogens**

3

4 Stephen A. Goldstein^{1*†}, Joe Brown^{*1}, Brent S. Pedersen¹, Aaron R. Quinlan¹, Nels C. Elde^{1†}

5

6 ¹Department of Human Genetics, University of Utah, Salt Lake City, UT, USA.

7 *Contributed equally.

8 [†]Corresponding authors.

9 Email: sgoldstein@genetics.utah.edu (S.A.G)

10 nelde@genetics.utah.edu (N.C.E)

11

12 **Abstract**

13 The ongoing SARS-CoV-2 pandemic is the third zoonotic coronavirus identified in the last
14 twenty years. Enzootic and epizootic coronaviruses of diverse lineages also pose a significant
15 threat to livestock, as most recently observed for virulent strains of porcine epidemic diarrhea
16 virus (PEDV) and swine acute diarrhea-associated coronavirus (SADS-CoV). Unique to RNA
17 viruses, coronaviruses encode a proofreading exonuclease (ExoN) that lowers point mutation
18 rates to increase the viability of large RNA virus genomes, which comes with the cost of limiting
19 virus adaptation via point mutation. This limitation can be overcome by high rates of
20 recombination that facilitate rapid increases in genetic diversification. To compare dynamics of
21 recombination between related sequences, we developed an open-source computational
22 workflow (IDPlot) to measure nucleotide identity, locate recombination breakpoints, and infer
23 phylogenetic relationships. We analyzed recombination dynamics among three groups of
24 coronaviruses with noteworthy impacts on human health and agriculture: SARS-CoV,
25 *Betacoronavirus-1*, and SADS-CoV. We found that all three groups undergo recombination with
26 highly diverged viruses from sparsely sampled or undescribed lineages, which can disrupt the
27 inference of phylogenetic relationships. In most cases, no parental origin of recombinant regions
28 could be found in genetic databases, suggesting that much coronavirus diversity remains
29 unknown. These patterns of recombination expand the genetic pool that may contribute to future
30 zoonotic events. Our results also illustrate the limitations of current sampling approaches for
31 anticipating zoonotic threats to human and animal health.

32

33

34 **Introduction**

35 In the 21st century alone three zoonotic coronaviruses have caused widespread human
36 infection: SARS-CoV in 2002 [1, 2], MERS-CoV in 2012 [2], and SARS-CoV-2 in 2019 [3]. Four
37 other coronaviruses, OC43, 229E, NL63, and HKU1 are endemic in humans and cause mild-to-
38 moderate respiratory disease with low fatality rates, though they may cause outbreaks of severe
39 disease in vulnerable populations [4-7]. Like SARS-CoV-2, SARS-CoV, and MERS-CoV, these
40 endemic viruses emerged from animal reservoirs. The origins of 229E and NL63 have been
41 convincingly linked to bats, much like the 21st century novel coronaviruses [8-10]. In a striking
42 parallel, both MERS-CoV and 229E appear to have emerged from bats into camelids,
43 established a new persistent reservoir, and then spilled over into humans [11-14]. In contrast,
44 the viral lineages that include OC43 and HKU1 originated in rodents [15,16], though very limited
45 rodent sampling leaves us with a poor understanding of the deep evolutionary history of these
46 viruses. Given the short infectious period of human coronavirus infections, the establishment of
47 endemicity was likely preceded by a period of intense and widespread transmission on regional
48 or global scales. In other words, SARS-CoV-2 is likely the fifth widespread coronavirus epidemic
49 or pandemic involving a still-circulating virus, though the severity of the previous four cannot be
50 reliably ascertained.

51 Livestock are similarly impacted by spillover of coronaviruses from wildlife reservoirs.
52 Three viruses closely related to OC43, bovine coronavirus (BCoV), equine coronavirus (ECoV)
53 and porcine hemagglutinating encephalomyelitis virus (PHEV) are enzootic or epizootic in cows,
54 horses, and pigs respectively [17]. Since 2017, newly emerged swine acute diarrhea syndrome-
55 associated coronavirus (SADS-CoV) has caused significant mortality of piglets over the course
56 of several outbreaks [18,19]. Sampling of bats proximal to impacted farms determined that
57 SADS-CoV outbreaks are independent spillover events of SADS_r(elated)-CoVs circulating in
58 horseshoe bats [20]. Molecular studies of SADS-CoV have identified the potential for further
59 cross-species transmission, including the ability to infect primary human airway and intestinal
60 cells [21,22].

61 Emergence of novel viruses requires access to new hosts, often via ecological
62 disruption, and the ability to efficiently infect these hosts, frequently driven by adaptive
63 evolution. Uniquely among RNA viruses, coronavirus genomes encode a proofreading
64 exonuclease that results in a significantly lower mutation rate for coronaviruses compared to
65 other RNA viruses [23,24]. This mutational constraint is necessary for maintaining the stability of
66 the large (27-32 kb) RNA genome but limits the evolution of coronaviruses via point mutation.
67 The high recombination rate of coronaviruses compensates for the adaptive constraints

68 imposed by high-fidelity genome replication [24,25]. The spike glycoprotein in particular has
69 previously been identified as a recombination hotspot [26]. Acquisition of new spikes may
70 broaden or alter receptor usage, enabling host-switches or expansion of host range.
71 Additionally, it may result in evasion of population immunity within established host species,
72 effectively expanding the pool of susceptible individuals. Recombination in other regions of the
73 genome is less well-documented but may also influence host range, virulence, and tissue
74 tropism, and likely contributed to the emergence of SARS-CoV [27,28].

75 To study the dynamics of recombination among clinically significant coronavirus lineages
76 we developed a novel web-based software, IDPlot, that incorporates multiple analysis steps into
77 a single user-friendly workflow. Analyses performed by IDPlot include multiple sequence
78 alignment, nucleotide similarity analysis, and tree-based breakpoint prediction using the GARD
79 algorithm from the HyPhy genetic analysis suite [29]. IDPlot also allows the direct export of
80 sequence regions to NCBI Blast to ease identification of closest relatives to recombinant regions
81 of interest.

82 Using IDPlot, we analyzed recombination events in three clinically significant lineages of
83 coronaviruses with sufficient samplings to conduct robust analyses: SARS-CoV-2-like viruses,
84 OC43-like viruses (*Betacoronavirus-1*) in the *Betacoronavirus* genus, and the SADSr-CoV group
85 of alphacoronaviruses. In all three groups, we found clear evidence of recombination resulting in
86 viruses with high overall nucleotide identity but exhibiting substantial genetic divergence in
87 discrete genomic regions. Recombination was particularly enriched around and within the spike
88 gene and 3' accessory genes. Within all three groups, recombination has occurred with
89 undescribed lineages, indicating that coronavirus diversity, even within these consequential sub-
90 groups of viruses, remains considerably undersampled. The potential for viruses to rapidly
91 acquire novel phenotypes through such recombination events underscores the importance of a
92 more robust and coordinated ecological, public health, and research response to the ongoing
93 pandemic threat of coronaviruses.

94

95 **Results**

96

97 **Coronavirus phylogenetic relatedness is variable across genomes**

98 Coronavirus genomes, at 27-32 kilobases (kb) in length, are among the largest known
99 RNA genomes, surpassed only by invertebrate viruses in the same *Nidovirales* order [30,31].
100 The 5' ~20 kb of the genome comprises open reading frames 1a and 1b, which are translated
101 directly from the genome as polyproteins pp1a and pp1ab and proteolytically cleaved into

102 constituent proteins (**Figure 1A**) [32]. Orf1ab is among the most conserved genes and encodes
 103 proteins essential for replication, including the RNA-dependent RNA-polymerase (RdRp), 3C-
 104 like protease (3C1Pro), helicase, and methyltransferase. Given the high degree of conservation
 105 in this region, coronavirus species classification is typically determined by the relatedness of
 106 these key protein-coding regions [33]. The 3' ~10 kb of the genome contains structural genes
 107 including those encoding the spike and the nucleocapsid proteins, as well as numbered

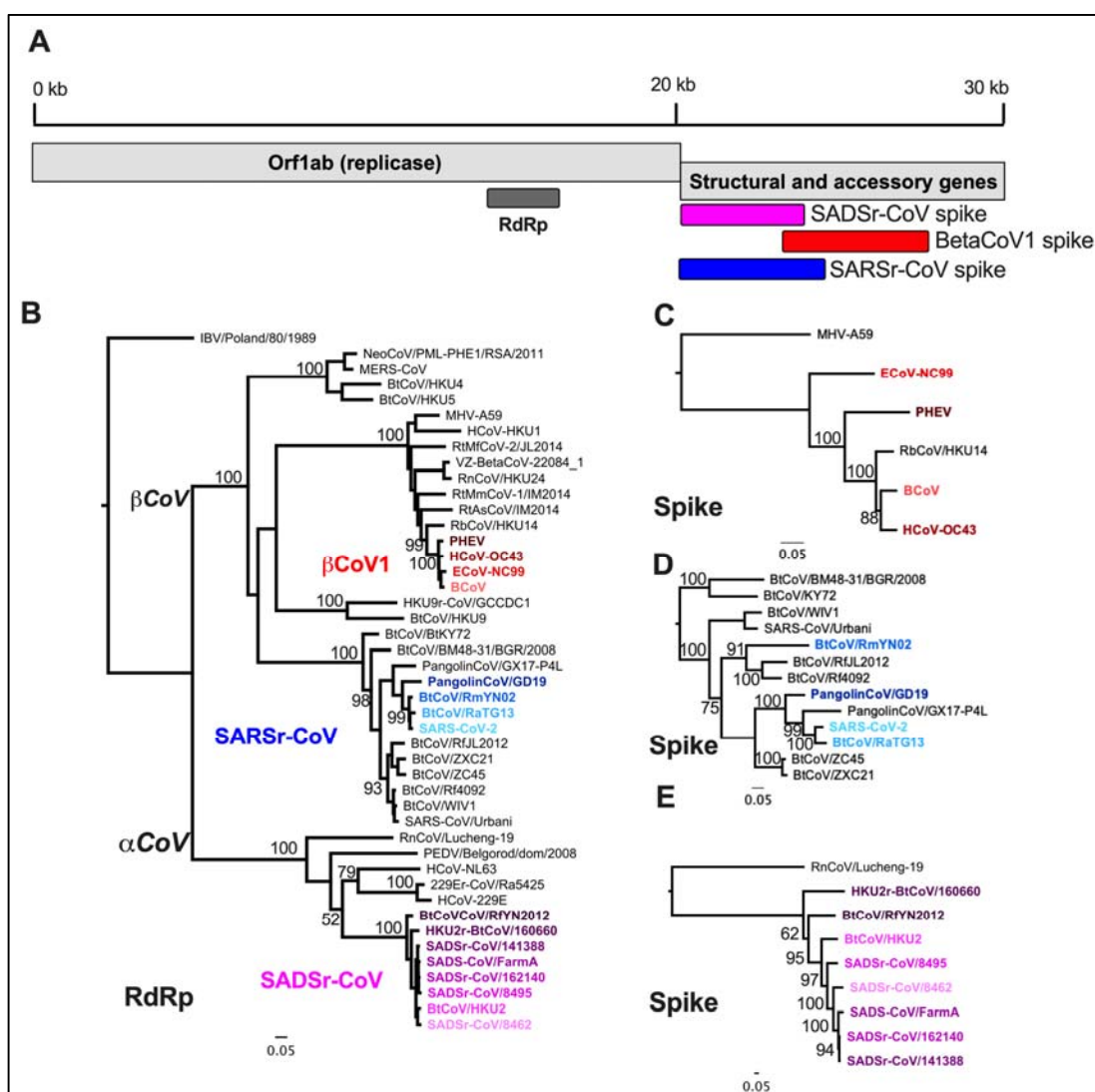


Figure 1. AlphaCoV and BetaCoV phylogenetic relationships are genome region-dependent. A)

Basic coronavirus genome organization with the 5' ~20 kb comprising the replicase gene that is proteolytically processed into up to 16 individual proteins. The 3' 10 kb comprises structural and genus-specific accessory genes. B) Maximum-likelihood (ML) phylogenetic tree of alpha and betaCoVs full-length RNA-dependent RNA-polymerase encoding region of Orf1ab. C) ML phylogenetic tree of full-length spike genes from SADS-related CoVs (magenta), rooted with the distantly related alphacoronavirus HCoV-229E D) ML phylogenetic tree of spike genes from viruses in the species *Betacoronavirus 1* (red) rooted with the distantly related betacoronavirus mouse hepatitis virus. E) ML phylogenetic tree of spike genes of SARSr-CoVs, with SARS-CoV-2-like viruses further analyzed in the paper highlighted in blue.

108 accessory genes that are unique to coronavirus genera and subgenera [34]. In contrast to the
109 relative stability of the replicase region of the genome, the structural and accessory region, and
110 in particular the spike glycoprotein, have been identified as recombination hotspots [26].

111 We set out to characterize the role of recombination in generating diversity across the
112 coronavirus phylogeny. A classic signature of recombination is differing topology and/or branch
113 lengths of phylogenetic trees depending on what genomic regions are analyzed. To identify
114 lineages of interest for recombination analysis, we built a maximum-likelihood phylogenetic tree
115 of full-length RdRp-encoding regions of representative alpha and betacoronaviruses, which
116 contain all human and most mammalian coronaviruses (**Figure 1B**). To further test whether
117 comparisons of RdRp sequence reflected ancestral relatedness, we conducted the same
118 analysis for the 3C1Pro and Helicase-encoding regions of Orf1ab (**Figure S2**). Phylogenetic
119 relationships were generally maintained in these trees and genetic relatedness remains very
120 high (90-99% within groups), which leads to some reshuffling with low bootstrap support. From
121 these trees we chose to further investigate the evolutionary dynamics of three clinically
122 significant groups of coronaviruses: SARS-CoV-2 like viruses (blue) from within *SARSr(related)*-
123 CoV, among which recombination has been reported though not characterized in detail,
124 endemic and enzootic OC43-like viruses of *Betacoronavirus-1* (*BetaCoV1*) (red), and SADSr-
125 CoVs (magenta). Although other coronavirus lineages are of public health interest, such as
126 those including the human coronaviruses HKU1, NL63, and 229E there is a relative paucity of
127 closely related sequences to these viruses, limiting our current ability to analyze these
128 genomes.

129 Within each group there is modest diversity revealed by comparing RdRp sequence: 94-
130 99% nt identity among the SADSr-CoVs, >97% nt identity within *Betacoronavirus-1*, and 91-
131 99% among the SARS-CoV-2-like viruses (**Figure S3**). Similar results were observed for 3C1Pro
132 and Helicase-encoding regions (**Figure S4**). In contrast, spike gene phylogenetic trees of each
133 group show greater diversity as illustrated by extended branch lengths and/or changes in tree
134 topology, suggesting either rapid evolution and/or recombination diversifies this region (**Figure**
135 **1B-D**). To analyze these possibilities, we developed a new pipeline to better study these
136 evolutionary patterns.

137

138 ***IDPlot Facilitates Nucleotide Identity and Recombination Analysis***

139 To investigate possible recombination-driven diversity among these viruses we
140 developed IDPlot, which incorporates several distinct analysis steps into a single Nextflow
141 workflow [35] and generates a comprehensive HTML report to facilitate interpretation and

142 downstream analysis. IDPlot combines existing algorithms into a single pipeline and provides a
143 statistically supported means to adjust recombination prediction and phylogenetic analysis in a
144 quickly interpretable visual display.

145 First, IDPlot generates a multiple sequence alignment using MAFFT (Figure 2A) [36]
146 with user-assigned reference and query sequences. In its default configuration, IDPlot then
147 generates a sliding window average nucleotide identity (ANI) plot, also displaying the multiple
148 sequence alignment with differences to the reference sequence (colored vertical lines) and gaps
149 (gray boxes) clearly highlighted. The plot is zoomable, and selected sequence regions can be
150 exported directly to NCBI BLAST. Users can also choose to run GARD, the recombination
151 detection program from the HyPhy suite of genomic analysis tools [29]. If GARD is implemented
152 (Figure 2B), distinct regions of the multiple sequence alignment are depicted between the
153 alignment and the ANI plot, and phylogenetic trees for each region are generated using
154 FastTree2 (Figure 2C) [37] and displayed (Figure 2E).
155

A significant barrier to effective use of GARD is that because it ultimately presents

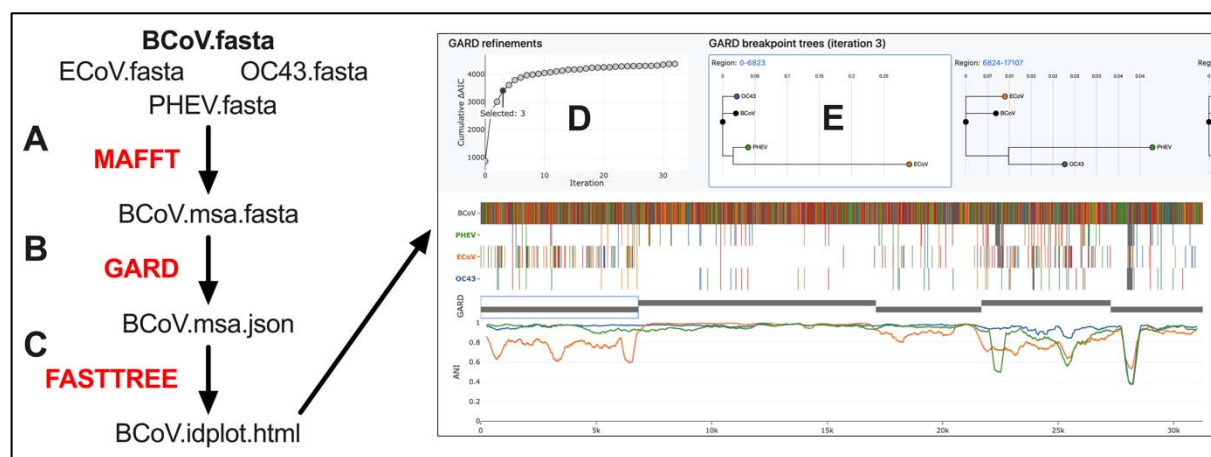


Figure 2. IDPlot workflow. IDPlot workflow. A) Reference and query sequences are aligned using MAFFT. B) Breakpoint detection is performed using GARD, capturing breakpoints across iterative refinements. C) Phylogenetic trees based on breakpoints from each iteration and are created using FastTree 2. D) Improvement in $\Delta\text{AIC-c}$ is plotted against the iteration E) Phylogenetic trees associated with the selected GARD iteration are displayed

156 multiple (sometimes dozens of) iterations, model choice and therefore the selection of
157 breakpoints for further analysis can be challenging. To alleviate this issue the IDPlot output
158 includes a graph showing a cumulative count of GARD's statistical iterations (Akaike information
159 criterion (AIC-c) on the y-axis) and the GARD model number on the x-axis (Figure 2D). GARD
160 uses $\Delta\text{AIC-c}$ for each proposed model to indicate the degree of fit improvement over the
161 preceding model, and this graph allows the user to easily determine when improvements
162 become increasingly marginal, which is often accompanied by prediction of spurious

163 breakpoints. Upon selection of a GARD iteration, the display switches to show the associated
164 phylogenetic trees (**Figure 2E**). Genomic regions are clickable, immediately bringing the
165 appropriate phylogenetic tree to the center of the display. Finally, the ability to export sequences
166 directly to BLAST enables the user to search for related sequences in GenBank, useful when
167 defined regions are highly divergent from the reference sequence or others included in the data
168 set under analysis.

169

170 **SARS-CoV-2-like virus recombination with distant SARSr-CoVs**

171 To test and validate IDPlot as a tool for examining the recombination dynamics of
172 coronaviruses, we initially conducted an analysis of SARS-CoV-2-like viruses within SARSr-
173 CoV. We chose these viruses as our initial IDPlot case study because recombination has been
174 previously described [38,39], though not characterized in great phylogenetic detail. This
175 provided the opportunity to evaluate IDPlot against a known framework but also advance our
176 understanding of the role recombination has played in the evolution of these clinically significant
177 viruses.

178 Prior to 2019 the SARS-CoV-2 branch within SARSr-CoV was known only from a single,
179 partial RdRp sequence published in 2016 [40]. Upon the discovery of SARS-CoV-2 this RdRp
180 sequence was extended to full genome-scale [3] and additional representatives from bats and
181 pangolins have since been identified [39] [41,42]. However, this singularly consequential lineage
182 remains only sparsely sampled and its evolutionary history largely obscured. Most attention on
183 these viruses to date has focused on the recent evolutionary history of SARS-CoV-2 with
184 respect to possible animal reservoirs and recombinant origins. Much less attention has been
185 paid to analyzing the evolution of known close relatives, the bat viruses RaTG13 and RmYN02,
186 and PangolinCoV/GD19.

187 Our IDPlot analysis does not support an emergence of SARS-CoV-2 via recent
188 recombination, consistent with previously published work [3] [38]. RaTG13 shows consistently
189 high identity across the genome with the only notable dip comprising the receptor-binding
190 domain in the C-terminal region of spike S1 (**Figure 3A**), which is proposed to originate via
191 either recombination or diversifying selection [38]. However, the still limited sampling in the
192 SARS-CoV-2-like lineage results in weak phylogenetic signals unable to distinguish between
193 rapid mutational divergence and recombination producing the low ANI in the RaTG13 receptor
194 binding domain.

195 In contrast, PangolinCoV/GD19 and RmYN02 show one and two significant drops in
196 ANI, respectively. Phylogenetic analysis of the PangolinCoV/GD19 recombinant region captures

197 the signal for both that virus (**Figure 3A, 3C, S5C**) and RmYN02 RR1, showing that both
 198 viruses fall onto separate branches highly divergent from SARS-CoV-2 and RaTG13 (**Figures**
 199 **3C**) with only 81% and 74% nucleotide identity to the closest sequences in GenBank,
 200 respectively (**Figure 3D, S5A**). These findings identify three unique spike genes among SARS-
 201 CoV-2 and its three closest known relatives (**Figure 3D**), indicative of recombination with
 202 SARSr-CoV lineages that remain to be discovered despite being the focus of intense virus
 203 sampling efforts over the last eighteen years, since the emergence of SARS-CoV.

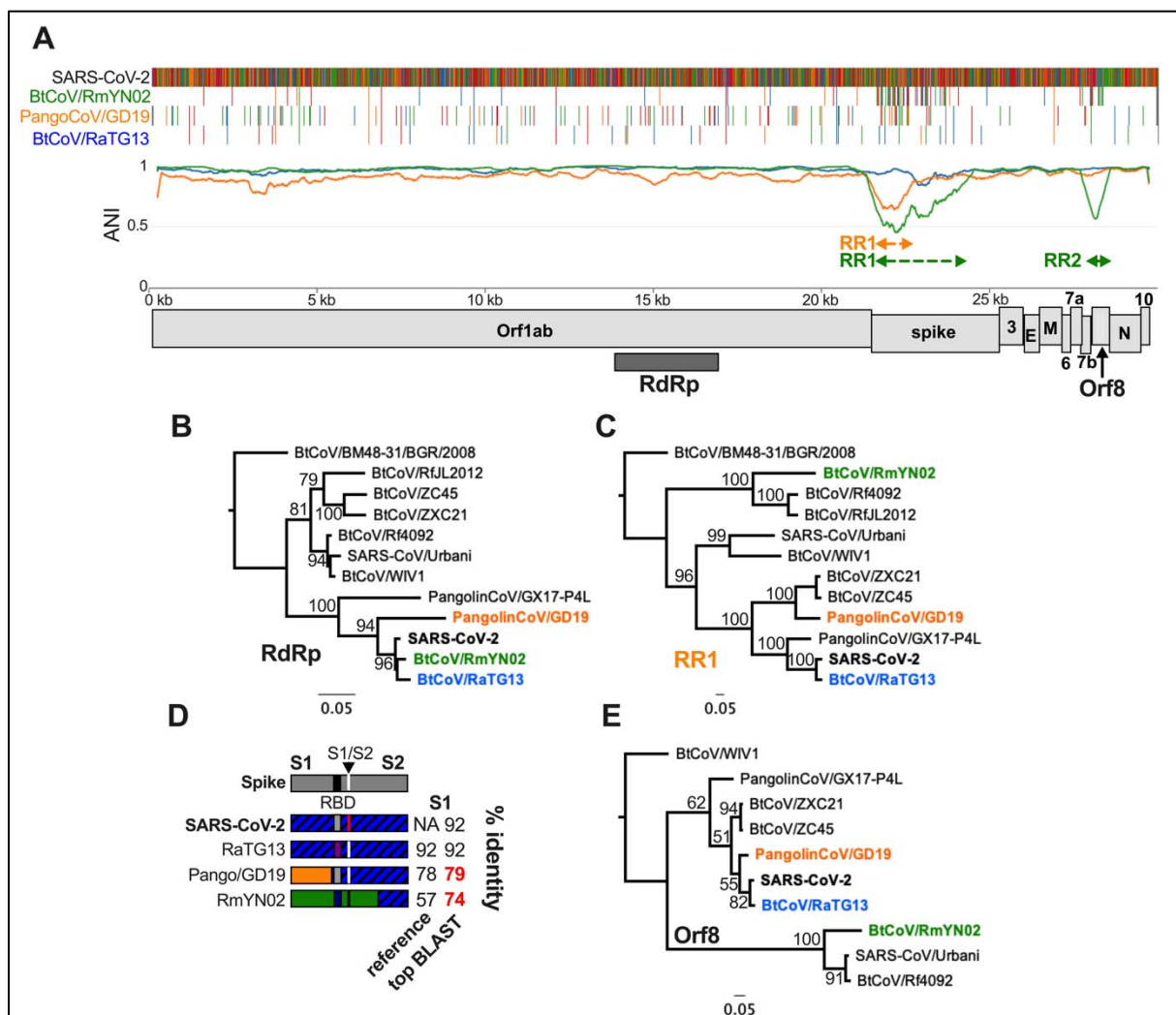


Figure 3. SARSr-CoV IDPlot Analysis. A) IDPlot analysis of SARS-CoV-2-like SARSr-CoVs with color-coded dashed lines defining divergent regions arising from recombination events with ancestral viruses. B) ML tree of the RdRp-encoding region of SARS-2-like and other SARSr-CoVs showing close relationship between the SARS-CoV-2 like viruses. C) ML tree of PangolinCoV/GD19 RR1 (which overlaps with BtCoV/RmYN02 RR1) showing different topology than the RdRp tree. D) Schematic of spike proteins indicating divergent regions and nucleotide identity to the reference sequence and closest related sequence in GenBank. E) ML tree of ORf8 showing that RmYN02 ORf8 is a divergent member of the SARS-CoV-like ORf8 branch.

204 In addition to spike, RmYN02 contains a second recombinant region that encompasses
 205 the 3' end of Orf7b and the large majority of Orf8 (**Figure 3A, S5A**). Orf8 is known to be highly

206 dynamic in SARSr-CoVs. SARS-CoV underwent an attenuating 29 nt deletion in Orf8 in 2002-
207 2003 [43] and Orf8 deletions have been identified in numerous SARS-CoV-2 isolates as well
208 [44-46]. In bat SARSr-CoVs intact Orf8 is typically though not always present but exhibits a high
209 degree of phylogenetic incongruence. Additionally, the progenitor of SARS-CoV encoded an
210 Orf8 gene gained by recombination [28,47]. The BtCoV/RmYN02 Orf8 has only 50% nt identity
211 to SARS-CoV-2 Orf8 and groups as a distantly related member of the branch containing SARS-
212 CoV (**Figure 3E**), exhibiting just 80% nucleotide identity to the closest known sequence.
213 Although the precise function of Orf8 is unknown, there is some evidence that like other
214 accessory proteins it mediates immune evasion [43]. Therefore, recombination in Orf8 has the
215 potential to alter virus-host interactions and may, like spike recombination, impact host range
216 and virulence.

217 This analysis confirmed that IDPlot allows us to characterize recombination events in
218 detail with a single workflow. We demonstrate that multiple SARS-CoV-2-like viruses have
219 recombined with unsampled SARSr-CoV lineages, limiting our ability to assess sources of
220 genetic diversification for these viruses. Under-sampling has implications limiting the
221 incisiveness of both laboratory and field investigations of these viruses.
222

223 **OC43-like viruses encode divergent spikes acquired from unsampled betacoronaviruses**

224 After validating IDPlot for recombination analysis of coronaviruses, we used it to
225 characterize recombination among the viruses in the *Betacoronavirus-1 (BetaCoV1)* group,
226 which includes the human endemic coronavirus OC43 and closely related livestock pathogens
227 bovine coronavirus (BCoV), equine coronavirus (ECoV), porcine hemagglutinating
228 encephalomyelitis virus (PHEV), and Dromedary camel coronavirus HKU23 (HKU23). Due to
229 the apparent low virulence of OC43 and limited sampling of the lineage, these viruses receive
230 relatively little attention outside agricultural research. However, this lineage has produced a
231 highly transmissible human virus, can cause severe disease in vulnerable adults, and is poorly
232 sampled [4]. An ancestral BCoV is believed to be the progenitor of the other currently
233 recognized *BetaCoV1* viruses with divergence dates estimated at 100-150 years ago for
234 OC43/PHEV [48] and 50 years ago for HKU23 [49]. Recombination with other
235 betacoronaviruses has been previously described for HKU23, so we excluded it from our
236 analysis [50]. The most closely related known virus to *BetaCoV1*, rabbit coronavirus HKU14
237 (RbCoV/HKU14) was reported to associate with ECoV in some regions [51], but no detailed
238 recombination analysis of the relationship between these viruses has been previously
239 described.

240 We conducted IDPlot analysis of OC43 and these related enzootic viruses of livestock
241 (**Figure 4A**) and identified at least six major recombination breakpoints in the ECoV genome.
242 The largest divergent region (Region 2) is >6 kilobases (**Figure 4A**). This region encompassing
243 ~20% of the genome exhibits only ~75% nt identity to the reference sequence, just ~81%
244 identity to any known sequence, and occupies a distant phylogenetic position relative to RdRp
245 (**Figure 4B-C, S6A, S6C-D**). In contrast to previous reports that ECoV clusters closely with
246 RbCoV/HKU14 in this region [51], our analysis reveals that this region of ECoV was acquired
247 via recombination from a viral lineage not documented in GenBank.

248 Striking variability in ANI within Region 2 led us to conduct a more detailed analysis.
249 IDPlot did not predict internal Region 2 breakpoints, so we conducted a manual analysis guided
250 by the IDPlot multiple sequence alignment, phylogenetic trees for each proposed sub-region,
251 and BLAST analysis to further dissect differing evolutionary relationships for sub-regions. We
252 found at least six and possibly seven distinct sub-regions (**Figure S7**). Nucleotide identity to top
253 BLAST hits of these sub-regions is highly variable (<70% to >90%), as is identity of the hits
254 themselves, with genetic contribution from RbCoV/HKU14-like viruses, BCoV-like viruses, and
255 more distant, uncharacterized lineages within the *Embecovirus* genus (**Figure S5**). Together,
256 this demonstrates that Region 2 was not acquired via a single recombination event but rather
257 represents a mosaic of known and unknown viral lineages that share an overlapping ecological
258 niche with ancestral ECoV.

259 Another major recombinant ECoV region, Region 6, includes the entire NS2 and HE
 260 genes as well as the majority of the spike gene (**Figure 4A, S6A**). Within this region on the
 261 multiple sequence alignment, we also identified a recombination event encompassing the
 262 majority of the PHEV spike gene, though this required downsampling (removing ECoV) to
 263 simplify the analysis (**Figure 4A, S6A**). Both ECoV Region 6 and the PHEV recombinant region
 264 occupy relatively distant nodes on a phylogenetic tree (**Figure S6G, J**) and exhibit <80%
 265 sequence identity to the reference sequence or any sequence in GenBank (**Figure S6A**),
 266 indicating they are derived from independent recombination events or diverged via repeated
 267 mutations. Recombination appears most likely given the even dispersion of low identity

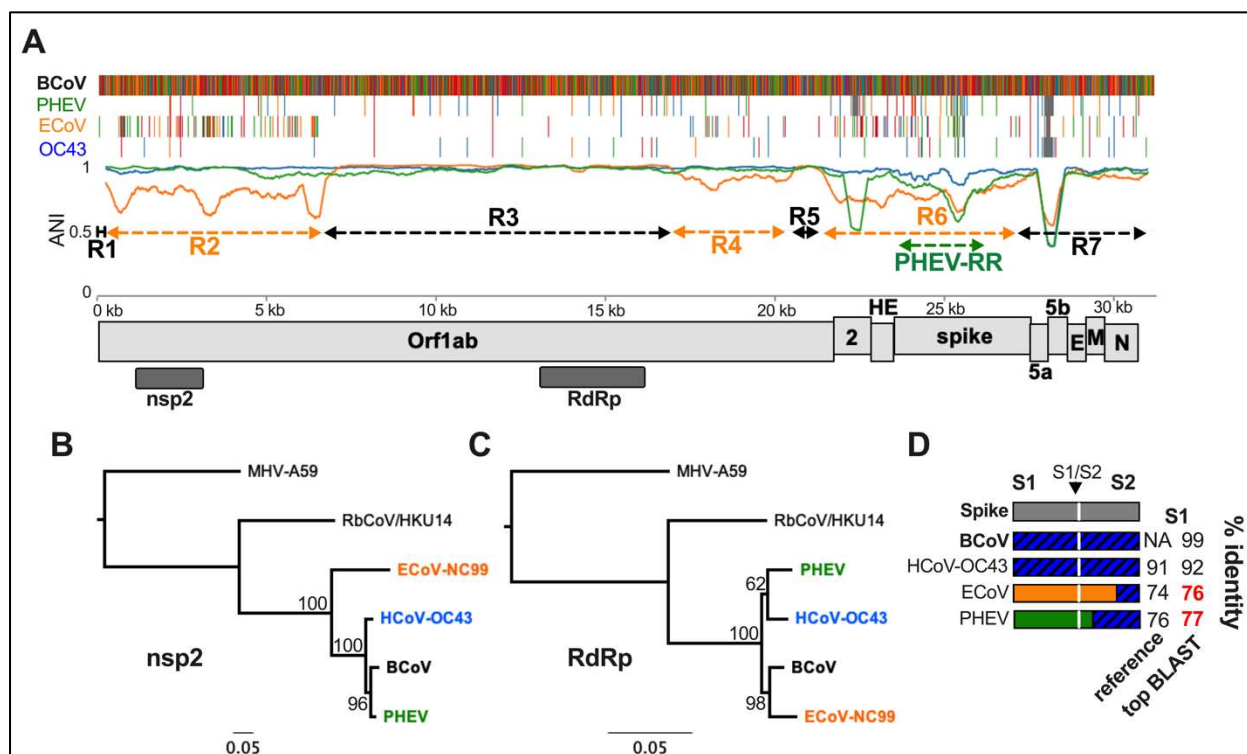


Figure 4. Recombination analysis of *Betacoronavirus-1*. A) Nucleotide identity plot and multiple sequence alignment of *Betacoronavirus-1* viruses. Orange dashed lines indicate divergent regions of the ECoV-NC99 genome while black dashed lines are regions with high identity to the reference sequence bovine coronavirus (BCoV). B) ML tree of nsp2-encoding region of Orf1ab, which falls within the divergent ECoV-NC99 Region 2. C) ML tree of the RdRp-encoding region of Orf1ab. D) Schematic depicting the spike gene diversity of *Betacoronavirus-1* demonstrating the divergence of ECoV-NC99 and PHEV. Top BLAST hits in bolded red indicate no GenBank entries with >80% nucleotide identity.

268 throughout the region, including in portions of the spike S2 domain which is otherwise highly
 269 conserved. Additional sampling might more definitively resolve these possibilities. Finally, we
 270 identified a third recombinant region, Region 4, in which ECoV exhibited high nucleotide identity
 271 with RbCoV/HKU14 (**Figure S4A, E**), further demonstrating the highly mosaic nature of the
 272 ECoV genome.

273 Our analysis of equine coronavirus offers a remarkable example of the degree and
274 speed of divergence facilitated by the high recombination rates among coronaviruses. Previous
275 genomic characterization of ECoV suggested that it is the most divergent member of *BetaCoV1*
276 based on nucleotide identity and phylogenetic positioning of full-length Orf1ab. However, in the
277 >10 kilobase Region 3 that accounts for ~1/3 of the entire genome (**Figure 4A**) ECoV exhibits
278 the highest nucleotide identity to BCoV in our dataset (98.5%) (**Figure 4A, S6D**), which is
279 inconsistent with it having diverged earlier than OC43 and PHEV. The latter viruses are
280 estimated to have shared a common ancestor with BCoV 100-150 years ago [48], suggesting
281 that all of the observed ECoV recombination has occurred more recently. Our discovery of
282 recombinant regions of unknown betacoronavirus origin suggest that unsampled, distantly
283 related lineages occupy overlapping ecological niches with ECoV and may continue to circulate
284 and participate in recombination events. Basal members of the subgenus that includes
285 *BetaCoV1* have been identified exclusively in rodents (**Figure 1B**), suggesting they are a
286 natural reservoir for these viruses. Although relatively little attention has been directed to these
287 viruses, studies of BCoV and ECoV cross-neutralization suggest population immunity to OC43
288 may provide only limited protection against infection mediated by these novel spikes [52]. No
289 recent zoonotic infections from this lineage have been documented, but the genomic collision of
290 these viruses with yet-undiscovered, presumably rodent viruses warrants a reassessment of
291 their potential threat to human health.

292

293 **SADSr-CoVs encode highly diverse spike and accessory genes**

294 In 2017 a series of highly lethal diarrheal disease outbreaks on Chinese pig farms were
295 linked to a novel alphacoronavirus, swine acute diarrhea syndrome-associated coronavirus
296 (SADS-CoV) [20,53], which is closely related to the previously described BtCoV/HKU2 [54].
297 Sampling of horseshoe bats nearby affected farms revealed numerous SADSr-CoVs with >95%
298 genome-wide nucleotide identity, suggesting porcine outbreaks were due to spillover from local
299 bat populations. To gain a better view of the genetic diversity among these viruses, we
300 conducted IDPlot analysis of a prototypical SADS-CoV isolate (FarmA) and seven bat SADSr-
301 CoVs sampled at different times before and after the first outbreaks in livestock (**Figure 5A**)
302 using bat SADSr-CoV/162140 as a reference sequence. Three notable observations emerged
303 from the identity plot: 1. Like ECoV, BtCoV/RfYN2012 exhibits evidence of recombination in the
304 5' end of Orf1ab 2. the spike region of the genome is highly variable as previously reported [20],
305 and 3. The 3' end of the genome also exhibits considerable diversity (**Figure 5A**).

306 To confirm the recent common ancestry of SADSr-CoVs in our data set we conducted
307 nucleotide identity and phylogenetic analyses of the RdRp, 3C1Pro, helicase, and
308 methyltransferase NTD-encoding regions of Orf1ab. All viruses exhibit exhibit 94-100%
309 nucleotide identity to the reference SADSr-CoV/162140 in these regions of the genome (**Figure**
310 **S4E-F, S8B-E, S9B-C**). In contrast, BtCoV/RfYN2012 recombinant region 1 (RR1) has <70%
311 identity to the reference or any known sequence (**Figure S8F, S9A**), providing evidence that an
312 uncharacterized alphacoronavirus lineage circulates in horseshoe bats, which frequently
313 recombines with SADSr-CoVs.

314 The spike gene is a striking recombination hotspot among SADSr-CoVs. Due to the
315 clustering of putative breakpoints surrounding the 5' end, 3' end, and middle of spike, we ran
316 IDPlot on subsets of three viruses – SADSr-CoV/162140 (reference), SADSr-CoV/141388 or
317 SADS-CoV/FarmA, and a virus of interest from the larger dataset. We found breakpoints
318 delineating six distinct and highly divergent spike genes among the eight analyzed viruses
319 (**Figure 5B**), which reflects recombination events encompassing either the entire spike or the
320 S1 subunit that mediates receptor binding. There are 3 unique full-length spikes
321 (BtCoV/RfY2012, HKU2r-BtCoV/160660, BtCoV/HKU2) with 63-73% nucleotide identity to the
322 reference sequence and two unique S1 domains (SADSr-CoVs/8462 and 8495) with <80%
323 identity to the reference (**Figure 5B, S9A**). Some of these regions match with high identity to
324 partial sequences in GenBank (indicated by an asterisk in Figure 5B) which may be either the
325 parent virus of the recombinant spike or different isolates of the same virus for which a full-
326 length genome is available. Other spikes in this dataset are clearly divergent from any other
327 known sequence.

328 In addition to spike, accessory proteins that target innate immunity can play important
329 roles in host range and pathogenesis [34]. We found a second recombination hotspot
330 surrounding the accessory gene Orf7a, which rivals spike gene diversification. Specifically, our
331 dataset contained five distinct Orf7a genes, some of which lack any closely related sequences
332 in GenBank (**Figure 5C, S9A**).

333 Finally, we mapped each inferred occurrence of a recombination event onto a SADSr-
334 CoV phylogenetic tree. SADSr-CoVs 141388 and 8495 share an Orf7a recombination event,
335 suggesting a recent common ancestor for these two viruses. The tree based on 3C1Pro was
336 most consistent with this evolutionary scenario (**Figure 5D**), while the other trees exhibit slightly
337 different topology with minimal diversity, likely due to cryptic recombination events among very
338 closely related viruses. Considering the 3C1Pro tree, it is evident that many independent

339 recombination events occurred in the very recent past given that few of the events are shared
340 among the viruses in our dataset (**Figure 5D**).

341 The SADSr-CoV lineage is rapidly diversifying via recombination, particularly in the spike
342 and ORF7a accessory genes. We observed that numerous viruses with >95-99% identity in
343 conserved Orf1ab regions contain highly divergent spike and accessory genes which may shift
344 host range and virulence in otherwise nearly isogenic viruses. These findings highlight how
345 viruses sampled to date represent only a sliver of circulating SADSr-CoV coronavirus diversity
346 and that coronaviruses can change rapidly, drastically, and unpredictably via recombination with
347 both known and unknown lineages. The SADSr-CoVs exemplify the potential of coronaviruses
348 to rapidly evolve through promiscuous recombination.

349

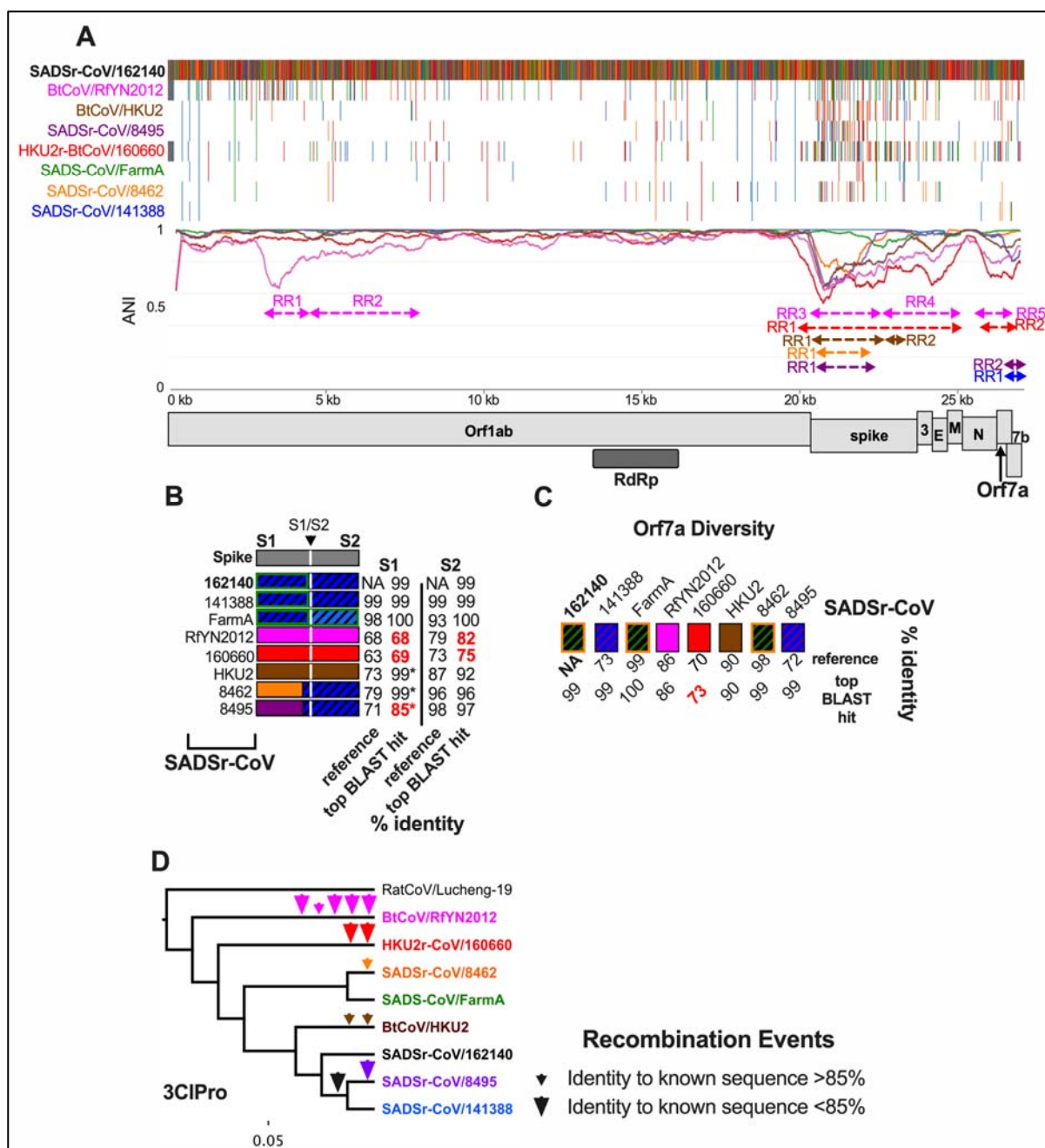


Figure 5. SADSr-CoV Analysis. A) IDPlot nucleotide identity and multiple sequence alignment of eight SADSr-CoVs. Color-coded dashed lines indicate divergent regions in corresponding viruses owing to recombination events. B) Schematic of spike genes of SADSr-CoVs along with nucleotide identity to the reference sequence and closest related sequences in GenBank for S1 and S2 domains. C) Schematic of Orf7a diversity with nucleotide identity to the reference sequence and closest related sequences in GenBank D) Phylogenetic tree of SADSr-CoVs based on 3C1Pro sequence illustrating the history of inferred recombination events indicated by arrowheads.

352 **Discussion**

353 We developed IDPlot to explore the role of recombination in the diversification of
354 coronaviruses. Coronaviruses are ubiquitous human pathogens with vast and underexplored
355 genetic diversity. SARS-CoV-2 is the second SARSr-CoV known to infect humans and the fifth
356 zoonotic coronavirus known to sweep through the human population following HCoVs 229E,
357 NL63, HKU1, and OC43 [9,10,15,48,55,56]. Most effort in evaluating the threat to human health
358 posed by coronaviruses has been dedicated to discovery of novel SARSr-CoVs in wildlife, yet
359 prior to the SARS-CoV-2 pandemic this group of viruses went largely undetected. Much less
360 attention has been paid to other groups that have produced human coronaviruses such as the
361 sparsely sampled *Betacoronavirus-1* and emerging livestock viruses such as the SADSr-CoVs,
362 which exhibit potential to infect humans and already have significant economic impacts.
363 Recombination detection can be difficult when parental viruses are unknown, as was revealed
364 with our analysis, due to difficulty in distinguishing between true recombination events versus
365 repeated mutations under strong selective pressure. Rapid evolution is most evident for spike
366 receptor binding domains, leading to polymorphism at critical residues [57,58]. Multiple
367 sequence alignments generated by IDPlot demonstrate that even in divergent spikes, the low
368 nucleotide identity is evenly distributed throughout putative recombinant regions. Additionally,
369 we see high divergence even in conserved regions such as Orf1ab and the spike S2 domain. In
370 all of these regions, including accessory genes, reshuffling of phylogenetic trees described in
371 our analysis provides strong evidence that recombination, not repeated individual mutations of
372 critical amino acid residues, accounts for the observed diversity.

373 We initially used the SARS-CoV-2-like viruses to test and validate IDPlot and in the
374 process characterized recombination among these viruses in greater detail than previously
375 reported. The observed variability in arrangements of PangolinCoV/GD19 and RmYN02 on a
376 SARSr-CoV phylogenetic tree (**Figure 3B-C, 3E, S5**) depending on the region being sampled is
377 a classic recombination signal easily observed in the IDPlot output. We also analyzed
378 recombination dynamics for viruses in *BetaCoV1* and among SADSr-CoVs. Broad similarities
379 emerge from these studies. Most recombination appears to involve the spike gene and/or
380 various accessory genes. However, in both *BetaCoV1* and among SADSr-CoVs we detected
381 recombination events in Orf1ab as well. Spike and accessory gene recombination events are
382 particularly notable given the potential to influence host range and pathogenesis.

383 This preliminary analysis showed that IDPlot is a powerful new pipeline for sequence
384 identity analysis, breakpoint prediction, and phylogenetic analysis. Existing workflows for
385 nucleotide similarity analysis are proprietary, lack the ability to identify phylogenetic

386 incongruence that is a signature of recombination and do not support direct export of genomic
387 regions for BLAST analysis. This automates and streamlines multi-step analysis with few
388 barriers to use. Nevertheless, there are opportunities for further improvement. Analysis of
389 recombination breakpoints implemented in GARD are of limited value for resolving unique
390 breakpoints in close proximity, as observed surrounding and within SADSr-CoV and other spike
391 genes, necessitating the use of small sets of sequences. Second, GARD is computationally
392 intensive and best suited to small data sets. It is configured as an optional step in IDPlot, so
393 multiple sequence alignments and nucleotide identity plots can be rapidly generated in a local
394 environment. However, for GARD analysis we relied on a high-performance computing cluster
395 to expedite the process. In the future, we anticipate adding other, less intensive breakpoint
396 prediction algorithms to the IDPlot options menu. Future advances in computational methods
397 may also improve the ability to resolve unique breakpoints clustered in genomic regions that are
398 recombination hotspots, most notably the spike gene.

399 Our IDPlot analyses revealed new evidence of extensive recombination-driven evolution
400 in other coronavirus groups. Wildlife sampling indicates that SADSr-Covs are a large pool of
401 closely related viruses circulating in horseshoe bat populations at high frequency. This is the
402 same genus of bats that include SARSr-CoVs suggesting that the ecological conditions for
403 SADSr-CoV spillover into humans may be in place. The relatedness of these viruses means
404 they have had little time to diverge via mutation, but we find they are rapidly diversifying due to
405 recombination, acquiring spike and accessory genes from unsampled viral lineages. These
406 findings demonstrate that rather than a single threat to human health posed by SADS-CoV,
407 there is a highly diverse reservoir of such viruses in an ecological position and with diversity
408 reminiscent of SARSr-CoVs. We found a similar dynamic at play among *BetaCoV1* which are
409 under-sampled to an even greater degree and receive far less attention. Nevertheless, these
410 viruses are involved in genetic exchange with unsampled lineages, with unpredictable
411 consequences.

412 Our findings bear on strategies for anticipating and countering future zoonotic events.
413 SARSr-CoVs garner considerable attention, with an intense focus on viruses able to infect
414 human cells using ACE-2 as an entry receptor. However, RmYN02 demonstrates that viruses
415 can toggle between spikes that recognize ACE-2 or different entry receptors but still infect the
416 same hosts and continue to undergo recombination. Work to prepare for future zoonotic SARSr-
417 CoVs must account for the possibility that the threat will come from coronaviruses only distantly
418 related to SARSr-CoVs undergoing frequent recombination and distributing genetic diversity
419 across the phylogenetic tree of coronaviruses.

420 More attention to the evolutionary dynamics of *BetaCoV1* and SADSr-CoVs is also
421 warranted. Both groups originate in wildlife: rodents and horseshoe bats respectively, and are
422 enzootic or epizootic in livestock. *BetaCoV1* includes a pandemic virus that swept the human
423 population, OC43, while SADS-CoV efficiently infects primary human respiratory and intestinal
424 epithelial cells [22]. Our ability to anticipate threats from both groups would benefit from
425 additional sampling, with *BetaCoV1* being particularly undersampled. Increased surveillance at
426 wildlife-livestock interfaces, including agricultural workers is needed for early detection of novel
427 viruses coming into contact with humans. Due to recombination, prior infection with a virus such
428 as OC43 cannot be presumed to be protective against even closely related viruses that can
429 encode highly divergent spikes, as demonstrated in our analysis. Similarly, efforts to develop
430 medical countermeasures against SADS-CoV should consider the full breadth of diversity
431 among related viruses, while aiming for broadly effective vaccines and therapeutics.

432 Using IDPlot, we identified extensive diversity among coronavirus spike and accessory
433 genes with potential implications for future pandemics. From the standpoint of understanding
434 coronavirus evolution, frequent recombination events often reshuffle phylogenetic trees and can
435 obscure evolutionary relationships. The extent to which viruses in current databases contain
436 genomic regions with no known close relatives makes clear that coronavirus diversity is vast
437 and poorly sampled, even for viruses circulating in well-studied locations. This proximity raises
438 the possibility of recurrent zoonoses of coronaviruses encoding divergent spike and accessory
439 genes. Therefore, preparedness efforts should consider a broad range of virus diversity rather
440 than risk a more narrow focus on close relatives of coronaviruses that most recently impacted
441 human health.

442

443 **Methods**

444

445 **Virus Sequences.** All sequences were downloaded from GenBank with the exception of
446 PangolinCoV/GD19 and BtCoV/RmYN02, which were acquired from the Global Initiative on
447 Sharing All Influenza Data (GISAID) database (<https://www.gisaid.org>).

448

449 **IDPlot.** IDPlot is initiated by the user designating reference and query sequences. A .gff3
450 annotation file can also be included in the input. The first step of IDPlot is multiple sequence
451 alignment using MAFFT [36] with default parameters. Size of the sliding window is customizable
452 and set to 500 for all of our analyses. For recombination analysis we ran GARD [29] as an
453 optional step, utilizing the multiple sequence alignment generated by MAFFT. Trees for each

454 GARD iteration are generated and displayed using Fast Tree 2 [37]. The entire output is then
455 exported into a chosen directory as idplot.html as well .json files containing raw GARD data.
456 More detailed information on IDPlot is available in the GitHub repository at
457 <https://github.com/brwnj/idplot>.

458
459 **Phylogenetic validation of breakpoints.** Putative breakpoints were further tested by
460 maximum-likelihood phylogenetic analysis using PhyML [59]. For *Betacoronavirus-1*,
461 RbCoV/HKU14 and MHV (as a root) were aligned with the four viruses in the IDPlot dataset. For
462 SADSr-CoVs we chose HCoV-229E as the root, with the exception of the spike gene, and
463 aligned it with the eight viruses in our dataset. We rooted the SADSr-CoVs with BtCoV/BM48-
464 31/BGR/2008. Given the better sampling of SADSr-CoV, we included more diversity in that
465 alignment to enhance phylogenetic signal. The signal for *BetaCoV1* and SADSr-CoV is
466 constrained by sampling limitations. We extracted breakpoint-defined regions from the
467 alignment and generated ML-phylogenetic trees using a GTR substitution model and 100
468 bootstraps. “Up” and “Dn” regions are the 500 nucleotides upstream or downstream of a
469 proposed 5’ or 3’ breakpoint, respectively. In the case of SADSr-CoV the clustering of
470 breakpoints around the 5’ and 3’ ends of spike precluded using unique Up and Dn regions for
471 each recombination event. Instead, we used the N-terminal section of nsp16 (MTase) and the M
472 gene, respectively. For BtCoV/RmYN02 RR2 and ORf8 phylogenetic testing we excluded
473 SADSr-CoVs that have a deletion in Orf8. RmYN02 UpRR2 also does not include BtCoV/WIV1
474 because it has a unique open reading frameed insert in this region and so does not align with
475 SADSr-CoVs lacking this Orfx.

476
477 **BLAST analysis.** To identify the source of recombinant regions we used NCBI Blastn with
478 default parameters, excluding the query sequence from the search. For SADSr-CoVs partial
479 spike sequences frequently appear as top hits. We included these, denoted by an asterisk in
480 reporting the results.

481
482 **Acknowledgements.** We thank E.C. Holmes and co-authors for the use of BtCov/RmYN02 and
483 PangolinCoV/GD19 genome sequences in our analysis. We thank Z.A. Hilbert for manuscript
484 assistance.

485
486
487

488 **References**

489

490 1. Drosten C, Günther S, Preiser W, van der Werf S, Brodt H-R, Becker S, et al.
491 Identification of a Novel Coronavirus in Patients with Severe Acute Respiratory
492 Syndrome. *The New England Journal of Medicine*. 2003;348: 1967–1976.
493 doi:10.1056/NEJMoa030747

494 2. Zaki AM, van Boheemen S, Bestebroer TM, Osterhaus ADME, Fouchier RAM. Isolation
495 of a Novel Coronavirus from a Man with Pneumonia in Saudi Arabia. *The New England
496 Journal of Medicine*. 2012;367: 1814–1820. doi:10.1056/NEJMoa1211721

497 3. Zhou P, Yang X-L, Wang X-G, Ben Hu, Zhang L, Zhang W, et al. A pneumonia outbreak
498 associated with a new coronavirus of probable bat origin. *Nature*. Nature Publishing
499 Group; 2020;579: 270–273. doi:10.1038/s41586-020-2012-7

500 4. Patrick DM, Petric M, Skowronski DM, Guasparini R, Booth TF, Krajden M, et al. An
501 Outbreak of Human Coronavirus OC43 Infection and Serological Cross-reactivity with
502 SARS Coronavirus. *Can J Infect Dis Med Microbiol*. Hindawi; 2006;17: 330–336.
503 doi:10.1155/2006/152612

504 5. Hand J, Rose EB, Salinas A, Lu X, Sakthivel SK, Schneider E, et al. Severe Respiratory
505 Illness Outbreak Associated with Human Coronavirus NL63 in a Long-Term Care Facility.
506 *Emerging Infectious Diseases*. 2018;24: 1964–1966. doi:10.3201/eid2410.180862

507 6. Zeng Z-Q, Chen D-H, Tan W-P, Qiu S-Y, Xu D, Liang H-X, et al. Epidemiology and
508 clinical characteristics of human coronaviruses OC43, 229E, NL63, and HKU1: a study of
509 hospitalized children with acute respiratory tract infection in Guangzhou, China. *Eur J Clin
510 Microbiol Infect Dis*. 2018;37: 363–369. doi:10.1007/s10096-017-3144-z

511 7. Killerby ME, Biggs HM, Haynes A, Dahl RM, Mustaquin D, Gerber SI, et al. Human
512 coronavirus circulation in the United States 2014–2017. *J Clin Virol*. 2018;101: 52–56.
513 doi:10.1016/j.jcv.2018.01.019

514 8. Pfefferle S, Oppong S, Drexler JF, Gloza-Rausch F, Ipsen A, Seebens A, et al. Distant
515 relatives of severe acute respiratory syndrome coronavirus and close relatives of human
516 coronavirus 229E in bats, Ghana. *Emerging Infectious Diseases*. 2009;15: 1377–1384.
517 doi:10.3201/eid1509.090224

518 9. Huynh J, Li S, Yount B, Smith A, Sturges L, Olsen JC, et al. Evidence supporting a
519 zoonotic origin of human coronavirus strain NL63. *Journal of Virology*. 5 ed. American
520 Society for Microbiology Journals; 2012;86: 12816–12825. doi:10.1128/JVI.00906-12

521 10. Tao Y, Shi M, Chommanard C, Queen K, Zhang J, Markotter W, et al. Surveillance of Bat
522 Coronaviruses in Kenya Identifies Relatives of Human Coronaviruses NL63 and 229E
523 and Their Recombination History. Perlman S, editor. *Journal of Virology*. American
524 Society for Microbiology Journals; 2017;91: 85. doi:10.1128/JVI.01953-16

525 11. Khalafalla AI, Lu X, Al-Mubarak AIA, Dalab AHS, Al-Busadah KAS, Erdman DD. MERS-
526 CoV in Upper Respiratory Tract and Lungs of Dromedary Camels, Saudi Arabia, 2013–
527 2014. *Emerging Infectious Diseases*. 2015;21: 1153–1158. doi:10.3201/eid2107.150070

528 12. Corman VM, Ithete NL, Richards LR, Schoeman MC, Preiser W, Drosten C, et al. Rooting
529 the phylogenetic tree of middle East respiratory syndrome coronavirus by
530 characterization of a conspecific virus from an African bat. *Journal of Virology*. American
531 Society for Microbiology Journals; 2014;88: 11297–11303. doi:10.1128/JVI.01498-14

532 13. Corman VM, Eckerle I, Memish ZA, Liljander AM, Dijkman R, Jonsdottir H, et al. Link of a
533 ubiquitous human coronavirus to dromedary camels. *Proc Natl Acad Sci USA*. National
534 Academy of Sciences; 2016;113: 9864–9869. doi:10.1073/pnas.1604472113

535 14. Crossley BM, Mock RE, Callison SA, Hietala SK. Identification and characterization of a
536 novel alpaca respiratory coronavirus most closely related to the human coronavirus 229E.
537 *Viruses*. Multidisciplinary Digital Publishing Institute; 2012;4: 3689–3700.
538 doi:10.3390/v4123689

539 15. Lau SKP, Woo PCY, Li KSM, Tsang AKL, Fan RYY, Luk HKH, et al. Discovery of a novel
540 coronavirus, China Rattus coronavirus HKU24, from Norway rats supports the murine
541 origin of Betacoronavirus 1 and has implications for the ancestor of Betacoronavirus
542 lineage A. Sandri-Goldin RM, editor. *Journal of Virology*. American Society for
543 Microbiology Journals; 2015;89: 3076–3092. doi:10.1128/JVI.02420-14

544 16. Wang W, Lin X-D, Guo W-P, Zhou R-H, Wang M-R, Wang C-Q, et al. Discovery, diversity
545 and evolution of novel coronaviruses sampled from rodents in China. *Virology*. Academic
546 Press; 2015;474: 19–27. doi:10.1016/j.virol.2014.10.017

547 17. Zhang J, Guy JS, Snijder EJ, Denniston DA, Timoney PJ, Balasuriya UBR. Genomic
548 characterization of equine coronavirus. *Virology*. 2007;369: 92–104.
549 doi:10.1016/j.virol.2007.06.035

550 18. Li K, Li H, Bi Z, Gu J, Gong W, Luo S, et al. Complete Genome Sequence of a Novel
551 Swine Acute Diarrhea Syndrome Coronavirus, CH/FJWT/2018, Isolated in Fujian, China,
552 in 2018. Matthijnssens J, editor. *Microbiol Resour Announc*. American Society for
553 Microbiology; 2018;7: 466. doi:10.1128/MRA.01259-18

554 19. Zhou L, Li QN, Su JN, Chen GH, Wu ZX, Luo Y, et al. The re-emerging of SADS-CoV
555 infection in pig herds in Southern China. *Transbound Emerg Dis*. John Wiley & Sons, Ltd;
556 2019;66: 2180–2183. doi:10.1111/tbed.13270

557 20. Zhou P, Fan H, Lan T, Yang X-L, Shi W-F, Zhang W, et al. Fatal swine acute diarrhoea
558 syndrome caused by an HKU2-related coronavirus of bat origin. *Nature*. 1st ed. Nature
559 Publishing Group UK; 2018;556: 255–258. doi:10.1038/s41586-018-0010-9

560 21. Yang Y-L, Qin P, Wang B, Liu Y, Xu G-H, Peng L, et al. Broad Cross-Species Infection of
561 Cultured Cells by Bat HKU2-Related Swine Acute Diarrhea Syndrome Coronavirus and
562 Identification of Its Replication in Murine Dendritic Cells In Vivo Highlight Its Potential for
563 Diverse Interspecies Transmission. Gallagher T, editor. *Journal of Virology*. American
564 Society for Microbiology Journals; 2019;93: 3134. doi:10.1128/JVI.01448-19

565 22. Edwards CE, Yount BL, Graham RL, Leist SR, Hou YJ, Dinnon KH, et al. Swine acute
566 diarrhea syndrome coronavirus replication in primary human cells reveals potential
567 susceptibility to infection. *Proceedings of the National Academy of Sciences*. National
568 Academy of Sciences; 2020;4: 202001046. doi:10.1073/pnas.2001046117

569 23. Eckerle LD, Lu X, Sperry SM, Choi L, Denison MR. High fidelity of murine hepatitis virus
570 replication is decreased in nsp14 exoribonuclease mutants. *Journal of Virology*. American
571 Society for Microbiology Journals; 2007;81: 12135–12144. doi:10.1128/JVI.01296-07

572 24. Denison MR, Graham RL, Donaldson EF, Eckerle LD, Baric RS. Coronaviruses: an RNA
573 proofreading machine regulates replication fidelity and diversity. *RNA Biol*. Taylor &
574 Francis; 2011;8: 270–279. doi:10.4161/rna.8.2.15013

575 25. Smith EC, Denison MR. Implications of altered replication fidelity on the evolution and
576 pathogenesis of coronaviruses. *Curr Opin Virol*. 2012;2: 519–524.
577 doi:10.1016/j.coviro.2012.07.005

578 26. Graham RL, Baric RS. Recombination, Reservoirs, and the Modular Spike: Mechanisms
579 of Coronavirus Cross-Species Transmission. *Journal of Virology*. 2010;84: 3134–3146.

580 27. Yang X-L, Hu B, Wang B, Wang M-N, Zhang Q, Zhang W, et al. Isolation and
581 Characterization of a Novel Bat Coronavirus Closely Related to the Direct Progenitor of
582 Severe Acute Respiratory Syndrome Coronavirus. Perlman S, editor. *Journal of Virology*.
583 American Society for Microbiology; 2016;90: 3253–3256. doi:10.1128/JVI.02582-15

584 28. Hu B, Zeng L-P, Yang X-L, Ge X-Y, Zhang W, Li B, et al. Discovery of a rich gene pool of
585 bat SARS-related coronaviruses provides new insights into the origin of SARS
586 coronavirus. *PLOS Pathogens*. Public Library of Science; 2017;13: e1006698.
587 doi:10.1371/journal.ppat.1006698

588 29. Kosakovsky Pond SL, Posada D, Gravenor MB, Woelk CH, Frost SDW. GARD: a genetic
589 algorithm for recombination detection. *Bioinformatics*. 2006;22: 3096–3098.

590 30. Saberi A, Gulyaeva AA, Brubacher JL, Newmark PA, Gorbatenya AE. A planarian
591 nidovirus expands the limits of RNA genome size. *PLOS Pathogens*. Public Library of
592 Science; 2018;14: e1007314. doi:10.1371/journal.ppat.1007314

593 31. Debat HJ. Expanding the size limit of RNA viruses: Evidence of a novel divergent
594 nidovirus in California sea hare, with a ~35.9 kb virus genome. 2018. doi:10.1101/307678

595 32. Fehr AR, Perlman S. Coronaviruses: an overview of their replication and pathogenesis.
596 *Methods Mol Biol*. New York, NY: Springer New York; 2015;1282: 1–23. doi:10.1007/978-
597 1-4939-2438-7_1

598 33. Coronaviridae Study Group of the International Committee on Taxonomy of Viruses. The
599 species Severe acute respiratory syndrome-related coronavirus : classifying 2019-nCoV
600 and naming it SARS-CoV-2. *Nature Microbiology*. Nature Publishing Group; 2020;5: 536–
601 544. doi:10.1038/s41564-020-0695-z

602 34. Liu DX, Fung TS, Chong KK-L, Shukla A, Hilgenfeld R. Accessory proteins of SARS-CoV
603 and other coronaviruses. *Antiviral Research*. 2014;109: 97–109.
604 doi:10.1016/j.antiviral.2014.06.013

605 35. Di Tommaso P, Chatzou M, Floden EW, Barja PP, Palumbo E, Notre Dame C. Nextflow
606 enables reproducible computational workflows. *Nat Biotechnol*. Nature Publishing Group;
607 2017;35: 316–319. doi:10.1038/nbt.3820

608 36. Katoh K, Misawa K, Kuma K-I, Miyata T. MAFFT: a novel method for rapid multiple
609 sequence alignment based on fast Fourier transform. *nar*. Oxford University Press;
610 2002;30: 3059–3066.

611 37. Price MN, Dehal PS, Arkin AP. FastTree 2 – Approximately Maximum-Likelihood Trees
612 for Large Alignments. Poon AFY, editor. *PLoS ONE*. Public Library of Science; 2010;5:
613 e9490. doi:10.1371/journal.pone.0009490

614 38. Boni MF, Lemey P, Jiang X, Lam TT-Y, Perry BW, Castoe TA, et al. Evolutionary origins
615 of the SARS-CoV-2 sarbecovirus lineage responsible for the COVID-19 pandemic.
616 *Nature Microbiology*. Nature Publishing Group; 2020;382: 1–10. doi:10.1038/s41564-020-
617 0771-4

618 39. Zhou H, Chen X, Hu T, Li J, Song H, Liu Y, et al. A Novel Bat Coronavirus Closely
619 Related to SARS-CoV-2 Contains Natural Insertions at the S1/S2 Cleavage Site of the
620 Spike Protein. *Current Biology*. Elsevier Ltd; 2020;: 1–12. doi:10.1016/j.cub.2020.05.023

621 40. Ge X-Y, Wang N, Zhang W, Hu B, Li B, Zhang Y-Z, et al. Coexistence of multiple
622 coronaviruses in several bat colonies in an abandoned mineshaft. *Virol Sin*. Springer
623 Singapore; 2016;31: 31–40. doi:10.1007/s12250-016-3713-9

624 41. Lam TT-Y, Jia N, Zhang Y-W, Shum MH-H, Jiang J-F, Zhu H-C, et al. Identifying SARS-
625 CoV-2-related coronaviruses in Malayan pangolins. *Nature*. Nature Publishing Group;
626 2020;583: 282–285. doi:10.1038/s41586-020-2169-0

627 42. Xiao K, Zhai J, Feng Y, Zhou N, Zhang X, Zou J-J, et al. Isolation of SARS-CoV-2-related
628 coronavirus from Malayan pangolins. *Nature*. Nature Publishing Group; 2020;583: 286–
629 289. doi:10.1038/s41586-020-2313-x

630 43. Muth D, Corman VM, Roth H, Binger T, Dijkman R, Gottula LT, et al. Attenuation of
631 replication by a 29 nucleotide deletion in SARS-coronavirus acquired during the early
632 stages of human-to-human transmission. *Sci Rep*. Nature Publishing Group UK; 2018;8:
633 990–15177. doi:10.1038/s41598-018-33487-8

634 44. Su YCF, Anderson DE, Young BE, Linster M, Zhu F, Jayakumar J, et al. Discovery and
635 Genomic Characterization of a 382-Nucleotide Deletion in ORF7b and ORF8 during the
636 Early Evolution of SARS-CoV-2. Schultz-Cherry S, editor. *mBio*. 2020;11: e01610–20.

637 45. Pereira F. Evolutionary dynamics of the SARS-CoV-2 ORF8 accessory gene. *Infect
638 Genet Evol*. Elsevier B.V; 2020;85: 104525–104525.

639 46. Young BE, Fong S-W, Chan Y-H, Mak T-M, Ang LW, Anderson DE, et al. Effects of a
640 major deletion in the SARS-CoV-2 genome on the severity of infection and the
641 inflammatory response: an observational cohort study. *The Lancet*. Elsevier; 2020;396:
642 603–611. doi:10.1016/S0140-6736(20)31757-8

643 47. Lau SKP, Feng Y, Chen H, Luk HKH, Yang W-H, Li KSM, et al. Severe Acute Respiratory
644 Syndrome (SARS) Coronavirus ORF8 Protein Is Acquired from SARS-Related
645 Coronavirus from Greater Horseshoe Bats through Recombination. Perlman S, editor.
646 *Journal of Virology*. 2015;89: 10532–10547. doi:10.1128/JVI.01048-15

647 48. Vijgen L, Keyaerts E, Lemey P, Maes P, Van Reeth K, Nauwynck H, et al. Evolutionary
648 history of the closely related group 2 coronaviruses: porcine hemagglutinating
649 encephalomyelitis virus, bovine coronavirus, and human coronavirus OC43. *Journal of*
650 *Virology*. 2006;80: 7270–7274. doi:10.1128/JVI.02675-05

651 49. Woo PCY, Lau SKP, Wernery U, Wong EYM, Tsang AKL, Johnson B, et al. Novel
652 betacoronavirus in dromedaries of the Middle East, 2013. *Emerging Infect Dis*. 2014;20:
653 560–572. doi:10.3201/eid2004.131769

654 50. So RTY, Chu DKW, Miguel E, Perera RAPM, Oladipo JO, Fassi-Fihri O, et al. Diversity of
655 Dromedary Camel Coronavirus HKU23 in African Camels Revealed Multiple
656 Recombination Events among Closely Related Betacoronaviruses of the Subgenus
657 Embecovirus. Pfeiffer JK, editor. *Journal of Virology*. American Society for Microbiology
658 Journals; 2019;93: 255. doi:10.1128/JVI.01236-19

659 51. Lau SKP, Woo PCY, Yip CCY, Fan RYY, Huang Y, Wang M, et al. Isolation and
660 characterization of a novel Betacoronavirus subgroup A coronavirus, rabbit coronavirus
661 HKU14, from domestic rabbits. *Journal of Virology*. 6 ed. 2012;86: 5481–5496.
662 doi:10.1128/JVI.06927-11

663 52. Nemoto M, Kanno T, Bannai H, Tsujimura K, Yamanaka T, Kokado H. Antibody response
664 to equine coronavirus in horses inoculated with a bovine coronavirus vaccine. *J Vet Med*
665 *Sci. JAPANESE SOCIETY OF VETERINARY SCIENCE*; 2017;79: 1889–1891.
666 doi:10.1292/jvms.17-0414

667 53. Gong L, Li J, Zhou Q, Xu Z, Chen L, Zhang Y, et al. A New Bat-HKU2-like Coronavirus in
668 Swine, China, 2017. *Emerging Infectious Diseases*. 2017;23: 1607–1609.
669 doi:10.3201/eid2309.170915

670 54. Lau SKP, Woo PCY, Li KSM, Huang Y, Wang M, Lam CSF, et al. Complete genome
671 sequence of bat coronavirus HKU2 from Chinese horseshoe bats revealed a much
672 smaller spike gene with a different evolutionary lineage from the rest of the genome.
673 *Virology*. Elsevier Inc; 2007;367: 428–439. doi:10.1016/j.virol.2007.06.009

674 55. Maganga GD, Pinto A, Mombo IM, Madjitetuyabé M, Mbeang Beyeme AM, Boundenga L,
675 et al. Genetic diversity and ecology of coronaviruses hosted by cave-dwelling bats in
676 Gabon. *Sci Rep. Nature Publishing Group*; 2020;10: 7314–13. doi:10.1038/s41598-020-
677 64159-1

678 56. Vijgen L, Keyaerts E, Moës E, Thoelen I, Wollants E, Lemey P, et al. Complete genomic
679 sequence of human coronavirus OC43: molecular clock analysis suggests a relatively
680 recent zoonotic coronavirus transmission event. *Journal of Virology*. American Society for
681 Microbiology Journals; 2005;79: 1595–1604. doi:10.1128/JVI.79.3.1595-1604.2005

682 57. Guo H, Hu B-J, Yang X-L, Zeng L-P, Li B, Ouyang S, et al. Evolutionary Arms Race
683 between Virus and Host Drives Genetic Diversity in Bat Severe Acute Respiratory
684 Syndrome-Related Coronavirus Spike Genes. Pfeiffer JK, editor. *J Virol*. 2020;94:
685 e00902–20.

686 58. Li F. Structure, Function, and Evolution of Coronavirus Spike Proteins. *Annu Rev Virol*.
687 Annual Reviews; 2016;3: 237–261. doi:10.1146/annurev-virology-110615-042301

688 59. Guindon S, Lethiec F, Dureux P, Gascuel O. PHYML Online—a web server for fast
689 maximum likelihood-based phylogenetic inference. *nar*. 2005;33: W557–W559.

690

691